Mechanical Systems and Signal Processing 99 (2018) 567–585

Contents lists available at ScienceDirect

Mechanical Systems and Signal Processing

journal homepage: www.elsevier.com/locate/ymssp

Nonlinear characterization of a Rossler system under periodic closed-loop control via time-frequency and bispectral analysis

Robert Bruce Alstrom [a,*], Stéphane Moreau [a], Pier Marzocca [b], Erik Bollt [c]

[a] Aeroacoustics Group, Department of Mechanical Engineering, University of Sherbrooke, Canada
[b] Aerospace Engineering and Aviation, School of Engineering, RMIT University, PO Box 71, Bundoora, VIC 3083, Australia
[c] Dept of Mathematics, Clarkson University, Potsdam, NY 13699-5815, United States

ARTICLE INFO

Article history:
Received 7 October 2016
Received in revised form 2 May 2017
Accepted 4 June 2017

Keywords:
Quadratic phase coupling
Nonlinear system identification
Bicoherence
Synchronization
Frequency entertainment

ABSTRACT

This study has two primary objectives; they are to investigate the nonlinear interactions (or quadratic phase-coupling) in a chaotic Rossler system under periodic closed-loop control via wavelet bispectral analysis; and to further identify the component mechanisms of synchronization. It is observed that a fixed-gain, fixed-frequency controller produces quadratic phase-coupling and decoupling along lines of constant frequency and that are perpendicular to the diagonal of the bicoherence matrix. Further, it was also observed that for synchronization to occur, *both* frequency entrainment and quadratic phase-coupling *must* be present. It was found that forcing the Rossler system with a constant frequency did not reduce the amplitude of the resulting period-1 orbit at sufficiently high gains. For the controller with a fixed gain and time-varying error signal, it was found that the time varying forcing frequency (adjusted by an extremum seeking feedback loop) linearizes the Rossler system and in doing so, suppresses the phase coherence completely. The time-varying forcing frequency removes the conditions for frequency entrainment by providing broadband attenuation; the result is suppression without synchronization.

1. Introduction

Power spectral analysis is sufficient for the analysis of linear systems, but they cannot provide information about the nonlinear interaction between Fourier modes, nor can they resolve the changes in Fourier components in time. In general, the bicoherence, which is the normalized bispectrum a measure of the amount of phase coupling that occurs in a signal or between two signals. Phase coupling is said to occur when two component frequencies are simultaneously present in the signal (s) along with their sum (or difference) frequencies and the phase of these component frequencies remains constant. There are two types of bicoherence analysis, the first is Fourier based and the other is wavelet based; the wavelet based option will be used in this research. A formal definition of wavelet bicoherence is provided in Section 3 of this work. Bispectral analysis is applied to a wide variety of nonlinear systems. These systems include mathematical nonlinear systems with quadratic and cubic nonlinearities, mechanical systems, aeromechanical systems and fluid mechanics. The following brief literature review will highlight some of these examples.

* Corresponding author.
E-mail addresses: Robert.Bruce.Alstrom@usherbrooke.ca (R.B. Alstrom), stephane.moreau@usherbrooke.ca (S. Moreau), pier.marzocca@rmit.edu.au (P. Marzocca), bolltem@clarkson.edu (E. Bollt).

http://dx.doi.org/10.1016/j.ymssp.2017.06.001
0888-3270/

Pezeshki et al. [1] performed a Fourier based auto-bispectral analysis on an unforced Rossler system with parameters a and b fixed at 0.2 and the parameter c was set at three discrete values of 2.6, 3.5 and 4.6. It was found that the nonlinear modal interactions were completely characterized by the bispectral analysis; this is due to the fact that the Rossler system equations contain a quadratic nonlinearity. For the period-1 motion ($c = 2.6$), it was found that spectrum contained a peak at 0.17 Hz and higher harmonics (typical for the Rossler system when the parameters are equal to 0.2). The corresponding bicoherence map showed self-coupling at 0.17 Hz and 0.34 Hz. For the period-2 motion ($c = 3.5$), it was observed that there is coupling between motions at the fundamental frequency and the period double frequency and its harmonics. It is the energy transfer between the fundamental and the period double frequency of 0.34 Hz that are responsible for the amplification of the frequency peaks seen in the spectrum. When the system is in the chaotic regime ($c = 4.6$), the bicoherence map actually fills with more contours and has similar features as the period doubling case. The analysis for this paper will be performed for $c = 5.7$. Classically, when the parameter c is set equal to 5.7, the Rossler system is simultaneously chaotic and phase coherent, making it more challenging to control.

In [1] a magnetically buckled beam was also studied. This mechanical system can be modeled as a Duffing's oscillator. A Duffing's oscillator is typically a second order system with a negative linear stiffness and a cubic nonlinearity. The Duffing oscillator is driven by a periodic forcing term in which the forcing frequency is fixed and the forcing amplitude is set equal to three values; each corresponding to a period-1, period-2 and chaotic regimes. The evolution of the bicoherence for the first two forcing amplitudes is similar to that of the Rossler system in that the quadratic phase-coupling appears to form along lines of constant frequency that match those found in the spectra. As the forcing amplitude increases, the 'bands' of bicoherence starts to increase in width; in the context of a forced system, quadratic phase coupling leads to the transfer of energy from the high frequency forcing to the lowest natural nonlinear frequency. This low frequency energy is then redistributed to many frequencies which eventually produce frequency spreading. The corresponding effect in the bicoherence matrix is the widening of the bands. Some nonlinear systems are self-excited, and as such the fundamental frequency will shed its energy to subharmonic, inter and superharmonic frequencies. When the Duffing oscillator is chaotic, the bicoherence map becomes diffuse and diminishes. This map feature is caused by the fact that nonlinearity is cubic; the influence of the cubic nonlinearity becomes stronger as the forcing amplitude is increased. Furthermore, the analysis method is of order two thus when the cubic nonlinearity becomes pronounced, it is possible for the magnitude of the bicoherence to have a value of zero. Auto and cross bispectral analyses of a two degree-of-freedom system with quadratic nonlinearities having a two-to-one internal (autoparametric) resonance are presented [2]. It was found that the bispectral analysis method characterized the nonlinear modal interaction both inside and out of the chaotic regime. Specifically, for the periodic orbits 1, 2, 8, 16 and the chaotic regime, all possessed strong bicoherence that originated primarily from the fundamental frequency of the system. There was negligible bicoherence observed between the amplitude modulations when in the chaotic regime. This bicoherence map feature may be typical of non-autonomous driven oscillators. It was also suggested that when there is little energy transfer between amplitude modulations, the modes are decoupled; if the frequency components are decoupled, then the system cannot exhibit a chaotic response. In Balachandran and Khan [3], a forced nonlinear oscillator and a set of coupled forced nonlinear oscillators with quadratic nonlinearities are studied. The main contribution of this work was that the method of scales was used to aid in the development of analytical approximations for the bispectra. The analytical relationships for the bispectra showed a dependence on phase and magnitude of the bispectra on various system parameters. Pasquali et al. [4] demonstrated both numerically and experimentally that higher order spectral analysis tools are able to identify structural nonlinearities in physics-based mechanical plate models (elastic and laminated) and experimental data.

Silva and Hajj [5] examined the experimental results from the High Speed Civil Transport (HSCT) Flexible Semispan Model. Using Fourier based bispectral analyses (auto and cross-bispectral analysis), they were able to study the nonlinear interactions between the structural deflections of the semispan model and the surface pressure fluctuations. This aeroelastic study provided a further insight into the nonlinear flutter mechanism. Chabalko presents an extensive application of both classical signal processing techniques and higher order spectral methods (both Fourier and Wavelet based) to study the hard flutter response of the HSCT and the F-16 Limit Cycle Oscillation [6]. Jamsek and his colleagues [13] extended the bispectral analysis technique to encompass a non-stationary version of the calculation called time-phase bispectral analysis. Time-phase couplings can be observed by additionally calculating the adapted bispectrum from which the time varying bi-phase and bi-amplitude can be obtained. The bi-phase and bi-amplitude provide a means by which one can distinguish the type of coupling i.e. linear or quadratic in a single measurement. Jamsek et al. then proceeded to test out the method on Poincare oscillators. Their frequency and phase relationships were examined at different coupling strengths, both with and without noise and later coupled van der Pol oscillators and cardio-respiratory signals [14]. In both works it was found that linear, quadratic and parametric (frequency modulated) interactions can generally be distinguished from one another. All the calculations in these two works are Fourier based.

Typically, systems under closed loop control are examined using classical methods. Gilliat and Strganac have suggested that it is not possible to design a controller than can decouple a nonlinear aeroelastic system [10]. Suppose, now that wavelet bispectral analysis could be used to design control laws which target the quadratic phase coupling between the Fourier components that cause instability like flutter? It should be noted that a review of the literature shows that quadratic phase coupling is key to both chaotic and periodic responses, but not explicitly discussed is the phenomena of frequency entrainment. In general, frequency entrainment occurs when a periodic force is applied to a system whose free response is the self-excited type. Specifically, entrainment can occur if the ratio between the forcing frequency and the natural frequency is in the vicinity of an integer or a fraction.

As such, this study has two objectives; the first is to identify the nonlinear interactions that result from the application of periodic closed-loop control; the second is to gain further insight into the constituent mechanisms that underlie the synchronization mechanism as it relates to nonlinear systems. This is accomplished by using wavelet bispectral analysis as a diagnostic and design tool to quantify the strength of the nonlinear modal interactions.

The current paper is organized as follows; the description of the problem is given in Section 2, followed by the methods of analysis in Section 3. Section 4 discusses the analysis of the un-controlled dynamics of the Rossler system. Section 5 presents the results of the *fixed gain-fixed frequency control law* and Section 6 present results on the *fixed gain, time-varying frequency control law*. The conclusions and future research directions are given in Section 7.

2. Problem description

To facilitate this study, the Rossler system will be used. The Rossler oscillator is the simplest chaotic system with continuous time, because it has a single quadratic nonlinear term, zx in its equations. The Rossler oscillator is used in this work because it exhibits chaotic behavior and phase coherence at the same time. The chaotic behavior is an analogy for turbulence. The Rossler oscillator equations are given as follows:

$$\dot{x} = -\Omega y - z + F_i(t) \tag{1}$$

$$\dot{y} = \Omega x + ay + F_i(t) \tag{2}$$

$$\dot{z} = b + z(x - c) + F_i(t) \tag{3}$$

where $\Omega = 1, a = b = 0.2$ and $c = 5.7$. These parameters yield a Rossler oscillator in the chaotic regime. Two forcing functions will be examined; they are written in the following manner:

$$F_1(t) = k[\sin \omega_f t - y(t)] \tag{4}$$

$$F_2(t) = k[\sin(\phi_f(\omega, t)) - y(t)] \tag{5}$$

The gain, k serves as a coupling parameter which scales the error signal and defines the amplitude. The error signal consists of the desired periodic orbit and the integrated state $y(t)$. For the first forcing function (Eq. (4)), the frequency ω_f is set equal to 0.34 Hz, the second harmonic of the Rossler system for the given parameters (See Eqs. (1)–(3)). In Eq. (5), the argument ϕ_f, varies as function of frequency and time. This is accomplished by extremum seeking control law. The extremum seeking control law allows the system to track and search for the optimal forcing frequency. The extremum seeking controller (see figures in Appendix A) consists of two filters; a low-pass filter and a high-pass filter, an integrator and a signal generator which provides the controller with periodic persistent excitation. The output/displacement signal from the Rossler oscillator is used as an input to the controller; it is passed to the high pass filter. The high pass filter removes the mean value but not the perturbation frequency, ω. The product of the filtered output and the zero mean sine signal leads to a zero mean signal as long as the maximum is not obtained. This signal is then passed to a low pass filter to extract the new mean value. The change of $\hat{\theta}$ due to integration is the result until the output, θ converges toward the optimal one. The choice of gain, cut-off frequencies, amplitude and frequency of the signal determines the speed of convergence. The reader is directed to Ariyur and Krstic [7] as they have provided a rigorous first proof of stability for general nonlinear systems. For both forcing functions, the gain/coupling parameter, k is adjusted manually.

3. Methods of analysis

The analysis performed in this work is accomplished using classical signal processing methods and wavelet based *time-frequency* and *bispectral analysis*. Many references have covered the classical signal processing techniques and they will not be covered here. Only the wavelet based methods will be discussed. Time-frequency analysis is concerned with identifying and quantifying oscillatory components present in real-life signals. This is achieved by projecting the signal onto the time-frequency plane, which enables one to study the properties of the signal in time and frequency at the same time. These projections are called time-frequency representations (TFRs). The time frequency representation used in this work is the spectrogram. The analysis in this paper utilizes the wavelet transform. The continuous wavelet transform has logarithmic frequency resolution. The wavelet transform of a function $s(t)$ is defined as:

$$W(\xi, \tau) = \int_{-\infty}^{+\infty} s(t)\psi^*_{\xi,\tau}(t)dt \tag{6}$$

where ξ and τ are scale and time variables respectively; $\psi^*_{\xi,\tau}(t)$ represents the wavelet family generated by continuous translations and dilations of the mother wavelet. The translations and dilations are obtained by:

$$\psi_{\xi,\tau} = \frac{1}{\sqrt{\xi}}\psi\left(\frac{t-\tau}{\xi}\right) \tag{7}$$

The wavelet to be used for this analysis is the log-normal wavelet. It is defined as follows:

$$\psi(t) = e^{-\frac{2\pi f_o \log t}{2}} \tag{8}$$

In this definition, f_o is chosen to be 3. This wavelet transform is the basis for the time-frequency and bispectral analysis. Wavelet bicoherence is a measure of quadratic phase-coupling in a single signal or between two signals (cross-bicoherence). Quadratic Phase Coupling (QPC) is said to have occurred when two frequencies f_1 and f_2, are present in the signal at the same time along with the sum (or difference) of the two frequencies and the sum of phases of these frequencies remains constant. The magnitude of the bicoherence ranges between zero and unity; complete quadratic phase-coupling happens when the bicoherence is one or closed to one. The two Fourier components are decoupled when the bicoherence magnitude is close

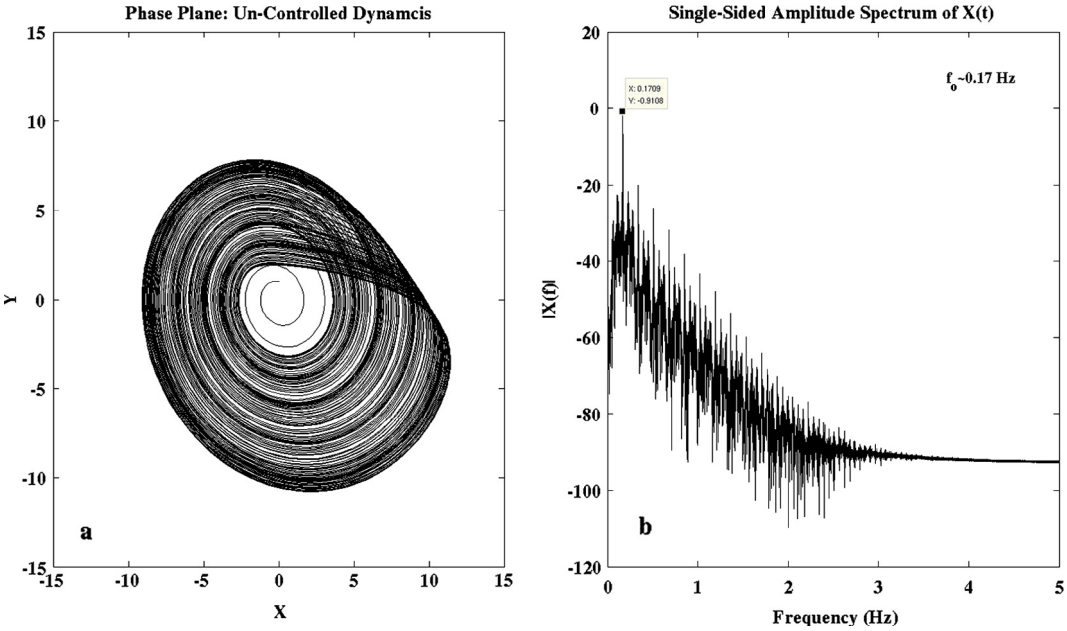

Fig. 1. Frequency spectrum of the un-controlled Rossler dynamics.

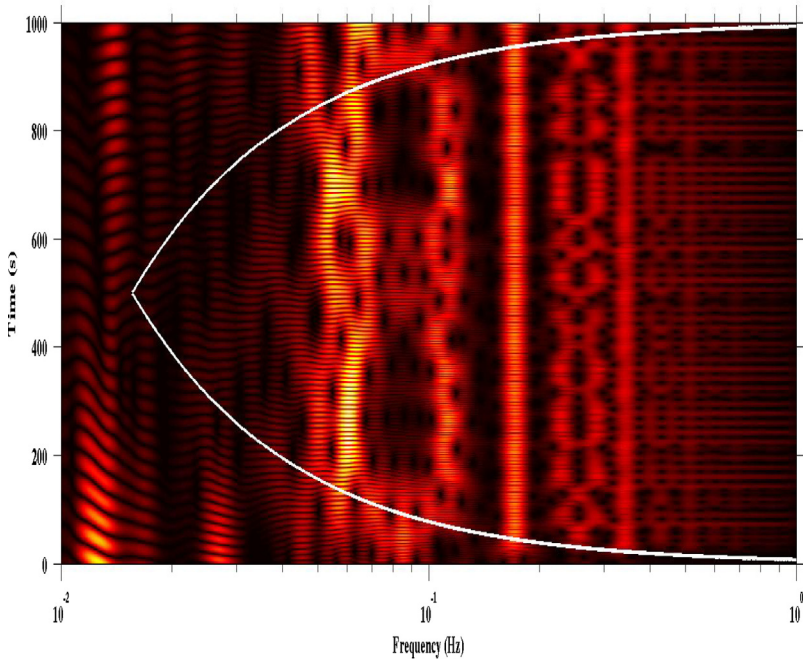

Fig. 2. Spectrogram (Un-controlled Rossler Dynamics).

to zero or equal to zero. If the nonlinearity is greater than order 2, then it is also possible to obtain zero magnitude for the bicoherence and higher-order spectra has to be investigated to unveil higher-order phase-coupling. The wavelet based spectral moment to be used in this analysis is an auto-bicoherence and is defined as follows:

$$|b^{w}_{xxx}(\xi_1,\xi_2)|^2 = \frac{|B^{w}_{xxx}(\xi_1,\xi_2)|^2}{\left(\int_T |W_x(\xi_1,\tau)W_x(\xi_2,\tau)|^2 d\tau\right)\left(\int_T |W_x(\xi,\tau)|^2 d\tau\right)} \tag{9}$$

where the scale xi is defined as $1/\xi = 1/\xi_1 + 1/\xi_2$, and $B^{w}_{xxx}(\xi_1,\xi_2)$ = int_T $W^{*}_{x}(\xi,\tau)\, W_x(\xi_1,\tau)\, W_x(\xi_2,\tau)\, d\tau$. The integration time, T, represents the interval of interest. Iatsenko et al. [11] developed MATLAB based tools producing windowed Fourier transforms, wavelet transform and their synchro-squeezed variants. The analysis in this paper utilizes the wavelet transform only. The advantage is that the wavelet based bicoherence calculation is less noisy that the Fourier counterpart. MATLAB was also used to compute both auto-bicoherence and cross-bicoherence. The phrases nonlinear modal interaction, quadratic phase-coupling and nonlinear interaction will be used interchangeably throughout this work.

4. Uncontrolled Rossler dynamics

The fast Fourier transform (FFT) of the un-controlled Rossler system shows that the fundamental frequency of the Rossler system in its chaotic regime is 0.17 Hz (Fig. 1). The frequency spectrum is broadband, but yet has very distinct frequency peaks. In fact, Farmer et al. [8] pointed out that strange attractors have power spectra that are superpositions of delta functions and broad backgrounds; this is what they call *phase-coherence*. The motion in the phase-plane, Fig. 1(a), takes place on an approximated closed curve which causes the sharp peak seen in Fig. 1(b). The presence of these frequency peaks will play a role in the mechanisms associated with synchronization. Stone [9] suggested that the Rossler system is self-frequency entrained. Stone showed by simulation experiment that for frequency entrainment to occur there must be a single strong frequency component, note however there are multiple strong peaks in a Rossler system in the chaotic regime.

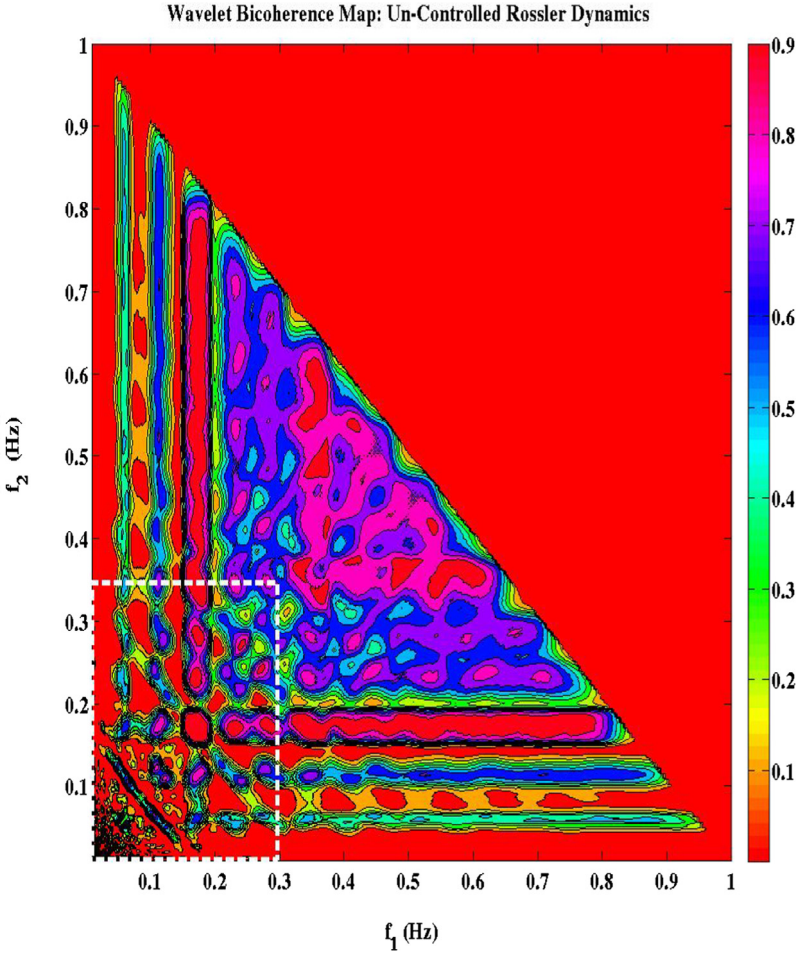

Fig. 3. Wavelet Bicoherence map (Uncontrolled Rossler dynamics).

In the spectrogram the exchange of energy shows up as inter-spectral moments; inter-spectral moments are the features in the spectrogram that look like ladder rungs. They either join two lines of constant frequency together or when there is weak periodicity, they manifest as transient growths in the time-frequency space. The reader will see that there are white lines in the spectrogram that open the right; the area inside these lines are the wavelet transforms coefficients that are well resolved. The amplitude of the Rossler oscillator in the chaotic regime is heavily self-modulated and therefore provides more details about the frequency components present in the signal. As such, the amplitude of the system is passed through the wavelet-based time-frequency analysis to produce the spectrogram in Fig. 2. For the un-controlled dynamics, the spectrogram shows that there are two distinct tones at 0.17 Hz and 0.34 Hz. The spectrogram also reveals that there is a significant energy transfer between the frequency band located at/centered on 0.061 Hz and the tone located at 0.1102 Hz. The energy exchanges take place over three time intervals, first between 0–200 s, then between 400–600 s and again between 800–1000 s. The two closely spaced sub-harmonics between 0.17 Hz and 0.34 Hz (0.2346 Hz and 0.2801 Hz) exchange energy for the duration of the simulation run. According to the spectrogram, there does not seem to be any appreciable energy exchange between the tone located at 0.1102 Hz and the natural frequency at 0.17 Hz. Fig. 3 is a bicoherence map of the un-controlled dynamics of the Rossler oscillator. It is clear from Fig. 3, that the QPC is highly organized. This map feature indicates that for certain frequencies; the Rossler oscillator is strongly phase coherent. The map shows that from 0.2 Hz to 0.5 Hz, there is a significant level of quadratic phase-coupling and is broadband due to energy cascading effects. The lines that form the "L" shapes in the map correspond to the Fourier components found in the frequency spectra. The reader can clearly see the lines of concentrated bicoherence associated with the natural frequency at 0.17 Hz, 0.11 Hz and 0.07 Hz respectively, with the natural frequency having the highest magnitude of bicoherence. In the lower left corner of the map, it can be observed that there are lines of concentrated bicoherence that are perpendicular to the diagonal axis of the frequency plane. Lines A, B, C and D shown in Fig. 4, represent lines of constant frequency. Note also that according to the definition of quadratic phase coupling, these lines of constant frequency are the sum of frequencies whose magnitude

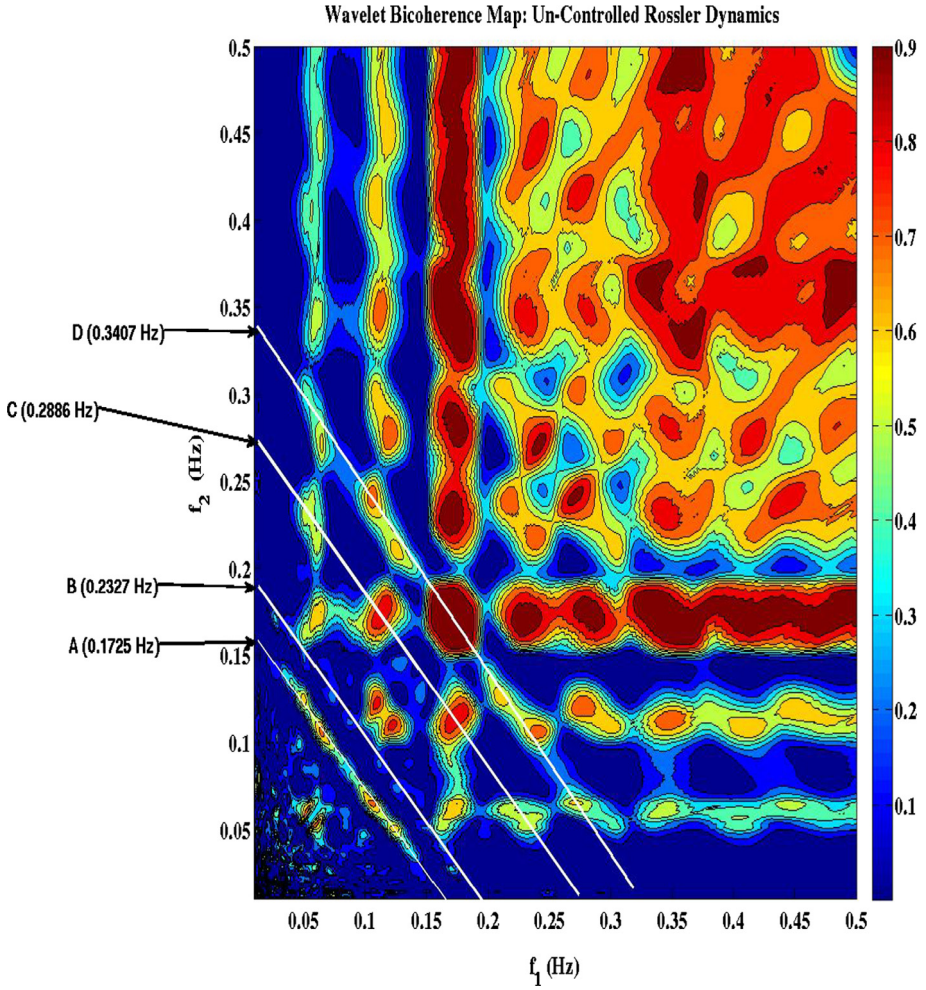

Fig. 4. Wavelet Bicoherence Map (Region inside white box, Fig. 3).

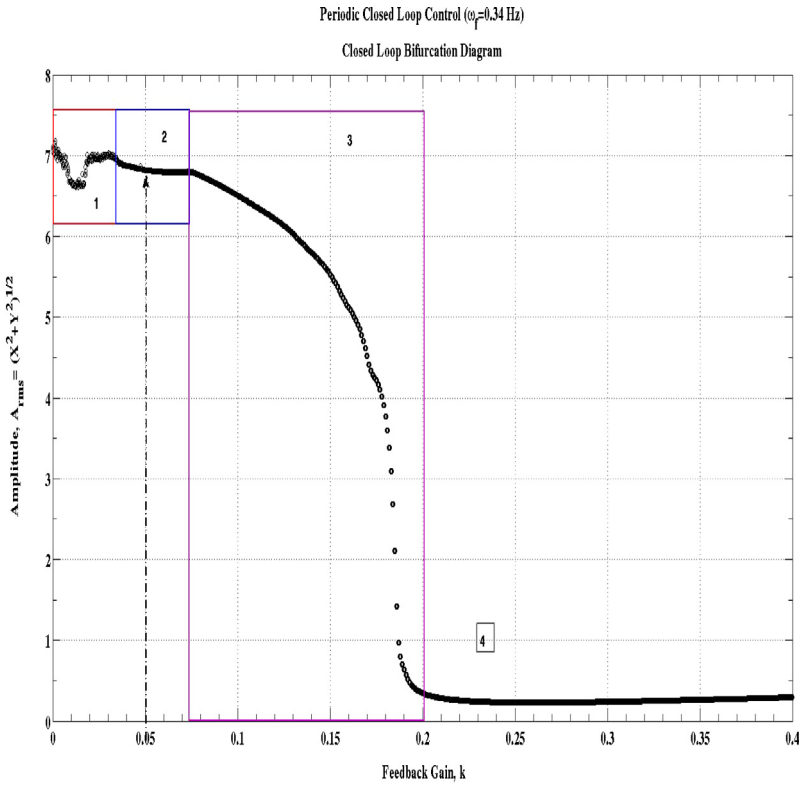

Fig. 5. Closed-loop Bifurcation diagram for controlled Rossler System.

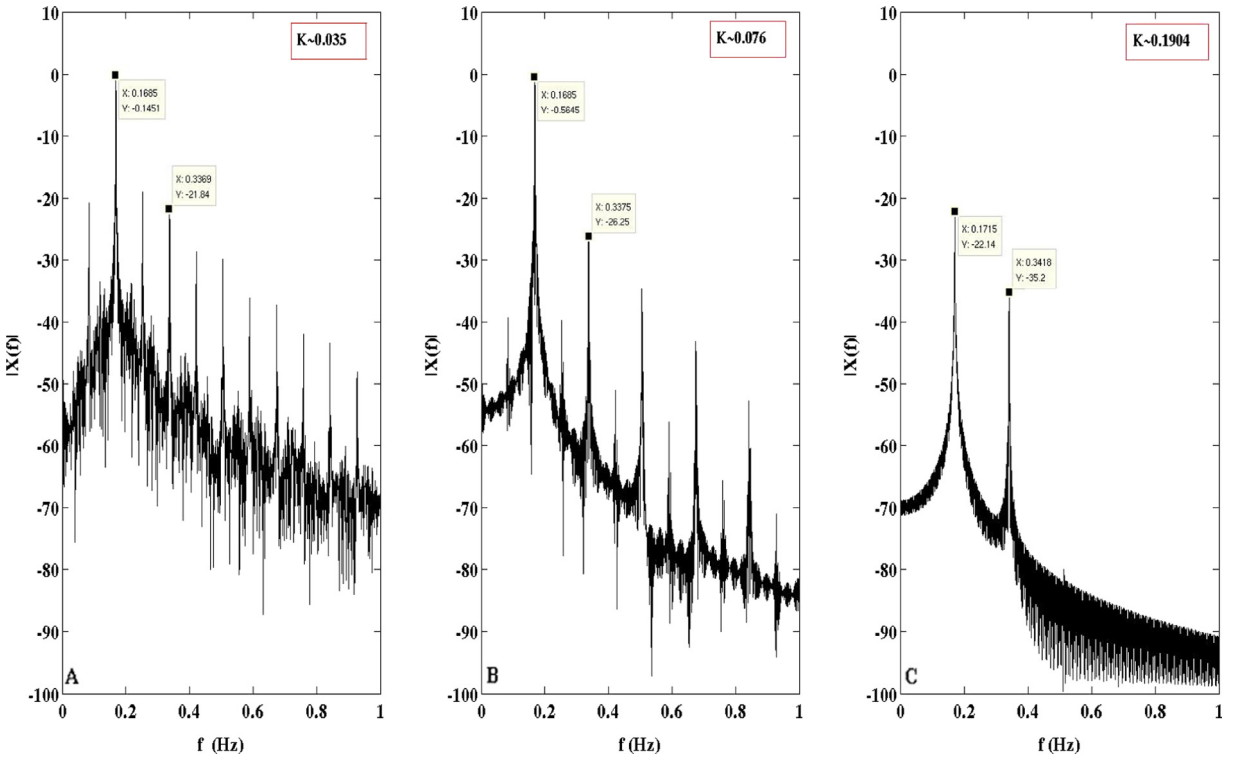

Fig. 6. Bifurcation Frequency spectra.

directly relates to the Fourier components seen in the FFTs. Line A is associated with ~0.17 Hz, Line B with ~0.23 Hz, Line C with ~0.29 Hz and Line D with 0.34 Hz.

In Fig. 4, Line A, the frequency triples show that there is an interaction between the tone at 0.1250 Hz and ~0.05 Hz. It was noted that in the time-frequency analysis there are energy exchanges between 0.1102 Hz and the frequency band centered about 0.061 Hz. The QPC ranges from 0.66 to 0.74 along Line A. For Line B, there is an interaction between 0.1270 Hz and 0.07 Hz. The bicoherence ranges from ~0.24 to 0.28. Just off Line B, there is a growth of nonlinear modal interaction that looks like two lobes. At this location on the bicoherence map, the QPC is 0.84 indicating that there is a significant energy exchange between 0.1102 Hz and 0.1220 Hz. Line B is centered on 0.2 Hz and the lobe is associated with the frequency 0.2327 Hz which is located between 0.17 Hz and 0.34 Hz in both frequency spectra (see Fig. 1(b)). Line C has a frequency of 0.2886 Hz and is again located between 0.17 Hz and 0.34 Hz. At Point 1 (Line C), the frequency components 0.2337 Hz and 0.05 Hz are coupled and the magnitude of the bicoherence is 0.56. At Point 2 (Line C), there is strong quadratic phase-coupling between the components 0.1748 Hz and 0.1164 (just off of 0.1102 Hz); the bicoherence at this intersection is 0.88. Line D is centered about 0.34 Hz, which is a higher harmonic. Along Line D, the most significant occurrence of quadratic phase-coupling takes place at a growth (in red) on the bicoherence map located between the vertical and horizontal components (also in red). This growth forms the vertex of the 'L' shape associated with the ~0.17 Hz tone. The red 'L' structure shows that there is strong self-coupling at ~0.17 Hz. The magnitude of the bicoherence at vertex is 0.99. The following section will present results on the effect of periodic closed-loop control on the quadratic phase-coupling.

5. Fixed-gain, fixed frequency control law

In this section, the results of a fixed gain-fixed frequency controller are presented. In order to understand how the controller affects the system, a closed-loop bifurcation diagram of the amplitude versus the coupling coefficient/gain is generated. The bifurcation diagram can be divided up into four regions, each identified by the numbers 1–4 in Fig. 5.

Region 1(R1) ranges from 0 to 0.035, Region 2 (R2) ranges from 0.035 to 0.076, Region 3 (R3) ranges from 0.076 to ~0.2 and Region 4 (R4) is any value of feedback gain greater than 0.2. In R1, the amplitude of the closed-loop system shows that

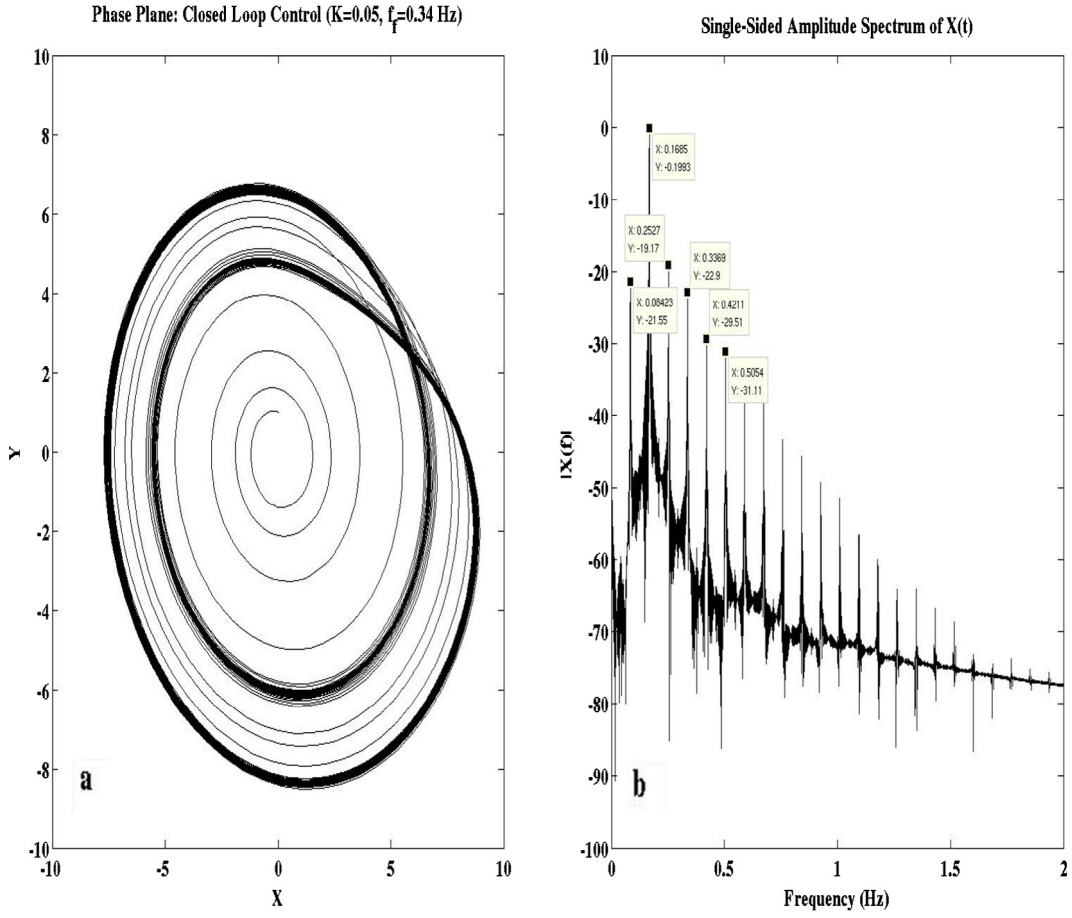

Fig. 7. Phase-plane & Frequency spectrum of the controlled Rossler system.

there is some variance when the gain is less than 0.035. At these low gains, the controller is not able to suppress the noise generated by the quadratic nonlinearity. Fig. 6(a) is the corresponding frequency spectrum. It is observed that the forced fundamental is shifted away from 0.17 Hz to 0.1685 Hz. The second harmonic is located at ∼0.3369 Hz (0.34 Hz, second harmonic and forcing frequency). Note that the phase coherence remains but the inter-harmonics begin to sharpen. For R2, the gain was increased to 0.076 and the variance in the amplitude has been eliminated. Fig. 6(b) shows that the frequency of the two tagged peaks has been preserved, but the power at the inter-harmonics are starting to decrease. In R3, the inter-harmonics and the higher harmonics are attenuated. This is confirmed by the spectrum in Fig. 6(c). The frequency peaks show a shift toward the fundamental at 0.17 Hz and 0.3418 Hz, the second harmonics. The larger amplitude at 0.17 Hz indicates that there is a long transient that eventually settles into a limit cycle at 0.3418 Hz. For values of the feedback gain, k greater than 0.2 (Region 4), the transient will be more damped and shorter in time. In the spectra, this shows a decrease in amplitude at 0.17 Hz and an increase in amplitude at ∼0.34 Hz. In the bifurcation diagram, note that the amplitude does not go to zero in R4; this means that as long as there is excitation at a constant frequency present with $k > 0.2$, there will always be a 'noise free' limit cycle present. The presence of a limit cycle is an indicator of synchronization.

Figs. 5 and 6 show that as the feedback gain, k is increased; the controlled Rossler undergoes a bifurcation sequence from chaotic to periodic. Throughout the bifurcation sequence, the Rossler system remains frequency entrained and phase coherent. There are two cases that will be discussed in this section in which the gain, k is fixed at 0.05 and 0.4 with the forcing frequency set at 0.34 Hz (second harmonic). The cases are also discussed extensively in [12].

For $k = 0.05$ and $\omega_f = 0.34$ Hz the phase-plane shows that the Rossler bands contract into two distinct bands (Fig. 7). The bands are made of closely spaced trajectories. The contraction in the phase space corresponds to the appearance of closely spaced subharmonic tones in the frequency spectra seen in the right panel of Fig. 7. These features seen in the frequency spectra are an indication of a transition from chaos to limit cycle motion. In the spectrogram of the amplitude (Fig. 8), it is observed that there are tones that correspond to those in the frequency spectra. They are located at 0.084 Hz, 0.1685 Hz (also in Fig. 7 (b)), 0.2536 Hz, 0.3375 Hz and 0.4212 Hz. The WT spectrum shows that there is frequency spreading over the range of frequencies from 0.01 Hz to 0.09 Hz. In the lower left corner of the bicoherence map (Fig. 9), it can be observed that there is strong quadratic phase-coupling from 0.01 Hz to 0.09 Hz. The magnitude of the bicoherence in this triangular region is greater than 0.85. Line A, is associated with the frequency ∼0.05 Hz and divides the triangular region of high bicoherence into two. Line B is associated with the frequency ∼0.1307 Hz, the highest magnitude of bicoherence along this line is 0.83. Line B, again divides the band of phase-coupling into two bounded regions where there is no appreciable quadratic phase-coupling i.e. the magnitude of the bicoherence is less than 0.1. Line C is associated with the frequency ∼0.2124 Hz. Line C is noticeably narrower than the band of bicoherence surrounding Line B. Line D is associated with the frequency ∼0.2936 Hz; the lowest magnitude of bicoherence along this line is ∼0.2. In order to get a better understanding of the growth patterns in the bicoherence

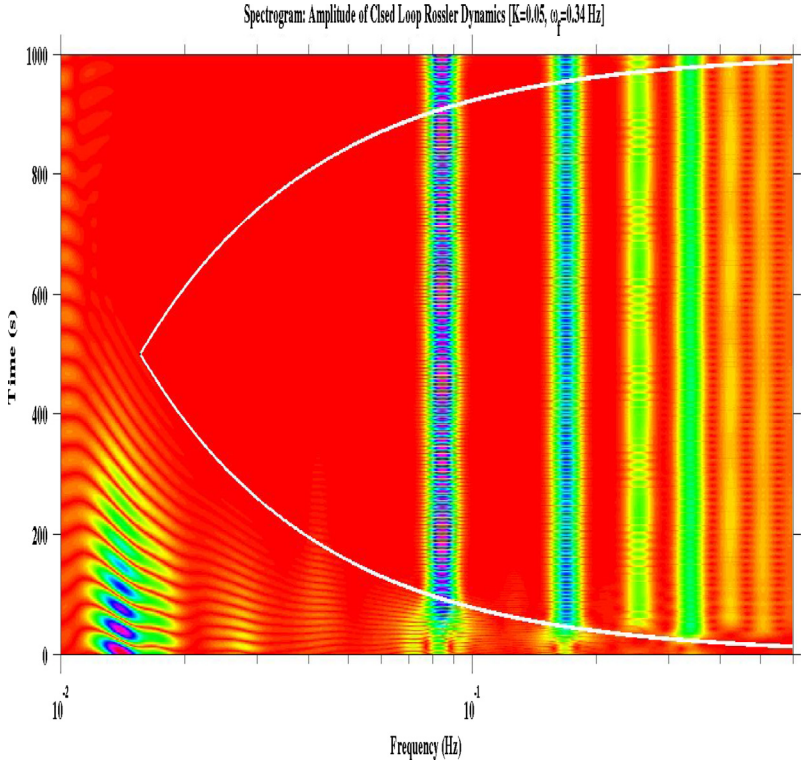

Fig. 8. Spectrogram of the Amplitude.

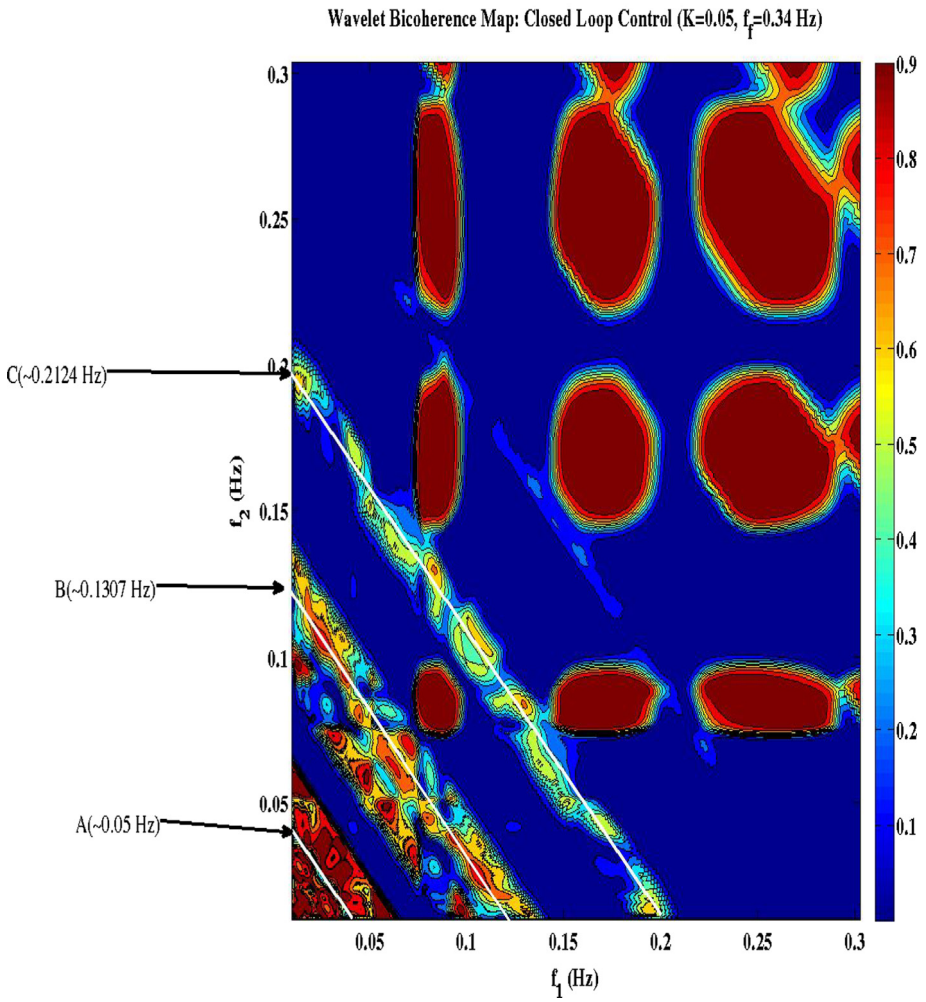

Fig. 9. Wavelet Bicoherence Map (k = 0.05 and ω_f = 0.34 Hz).

map, a plot of the diagonal of the bicoherence matrix was generated (Fig. 10). The diagonal of the bicoherence map is different from a frequency or power spectrum in that the diagonal bicoherence globally quantifies the quadratic phase-coupling between the components f_1 and f_2 at the frequency f_3. There are three bandwidths over which the magnitude of the bicoherence is significant (bicoherence is greater than 0.8). These bandwidths are centered about 0.1685 Hz (roughly equal to the fundamental of 0.17 Hz), 0.3374 Hz (close to second harmonic and forcing frequency at 0.34 Hz) and 0.5054 Hz (close to third harmonic 0.5121 Hz). The bandwidth with a peak at 0.5054 Hz shows the system is still phase coherent and chaotic at frequencies greater than 0.5054 Hz. The plot of the diagonal also shows that there are three bandwidths over which quadratic phase-coupling is either very weak or completely decoupled. These bandwidths are centered about ~0.085 Hz (close to sub-harmonic 0.062 Hz), ~0.2500 Hz (close to inter-harmonic 0.2813 Hz) and 0.4082 Hz (close to inter-harmonic 0.4010 Hz). The bandwidths are enclosed by the boxes in Fig. 10. The bandwidth centered about 0.25 Hz shows that the frequency components are completely decoupled (enclosed in the red box). For the control gain set equal to 0.05, it is observed that the levels of high bicoherence (strong self-coupling) are *directly centered* on the fundamental frequency, two higher harmonics and three sub-harmonics. The bandwidths where the system is weakly coupled and/or completely decoupled are centered on frequencies that are *close to* sub-harmonics and inter-harmonics. In the frequency spectrum of the uncontrolled Rossler oscillator (Fig. 1), the sub-harmonics and super-harmonics have very distinct, sharp peaks, and as such the condition for frequency entrainment is still present. It has been shown by simulation that the quadratic phase-coupling is highest about the spectral moments that cause frequency entrainment. Also, in the frequency spectrum of the uncontrolled Rossler dynamics; it is observed that there are two closely spaced inter-harmonics that repeat between each successive harmonic, the inter-harmonic peaks are not sharp, but rounded, as are the frequencies that are in close proximity to a subharmonic. Here, the experimental condition for frequency entrainment is not met. As a result, the quadratic phase-coupling over these bandwidths is less than 0.1. It is also clear that forcing the system with a fixed frequency results in the suppression of quadratic phase-coupling along lines of constant frequency that are perpendicular to the diagonal of the Bicoherence matrix.

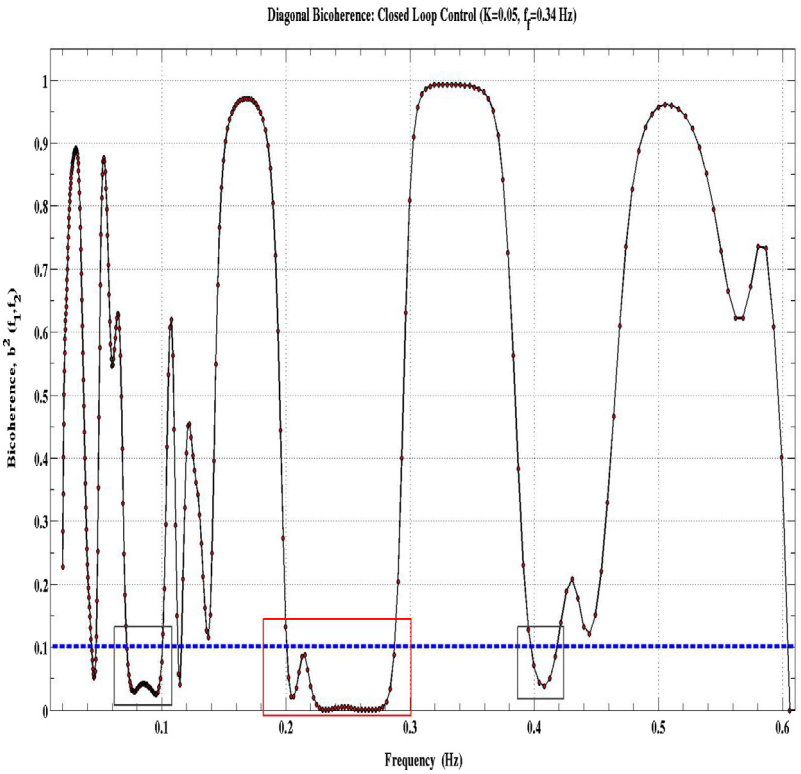

Fig. 10. Diagonal of the bicoherence matrix ($k = 0.05$ and $\omega_f = 0.34$ Hz).

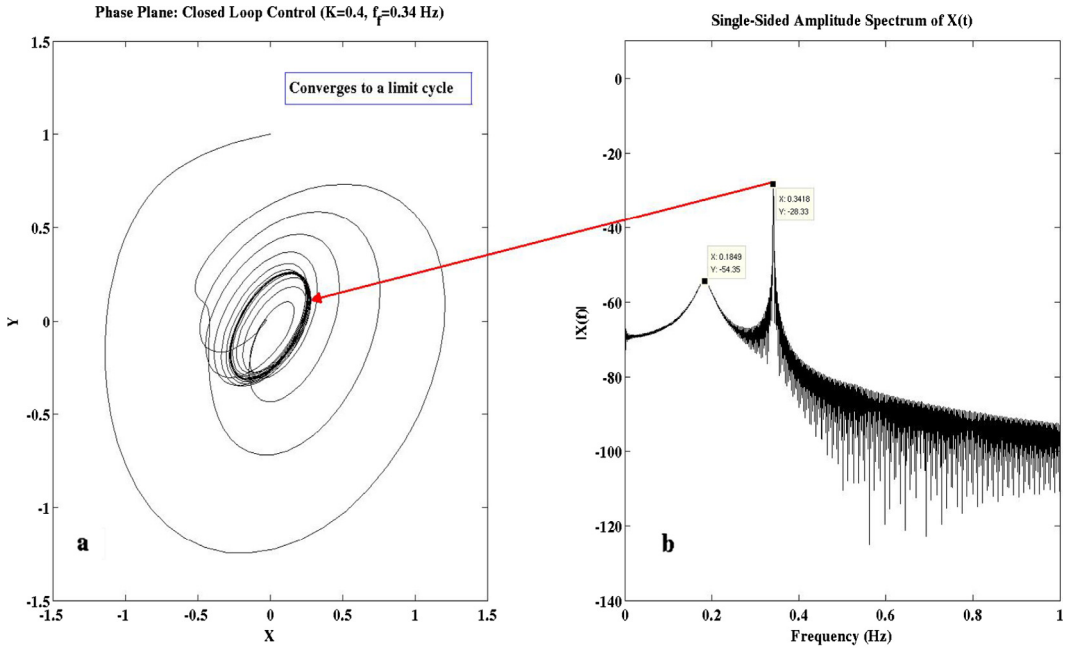

Fig. 11. Phase-plane & Frequency Spectrum ($k = 0.4$ and $\omega_f = 0.34$ Hz).

For the feedback gain set at 0.4, the phase-plane Fig. 11(a) shows that the transient converges to a limit cycle. The transient is responsible for the frequency spreading (centered about 0.1849 Hz) seen in the right panel of Fig. 11. The frequency of the limit cycle is 0.3418 Hz and has amplitude of 28.33 dB. The other harmonics have been completely attenuated as predicted by the closed-loop bifurcation diagram. The frequency spreading seen in the frequency spectrum correlates with the bandwidth along the diagonal (Figs. 12 and 13) that ranges from 0.025 Hz to ~0.3 Hz. The quadratic phase-coupling across

this bandwidth is generally above 0.8. There is a decoupling bandwidth from ~0.3 Hz to 0.4 Hz. The prescribed forcing frequency is 0.34 Hz at the center of the decoupling bandwidth. This is followed by a bandwidth (0.4–0.6 Hz, the upper limit is selected to magnify the regions of interest in the bicoherence map) in which the quadratic phase-coupling is not less than 0.5. Thus far, the results show that a bandwidth which contains decoupling removes the frequencies along which energy can be passed. Some conclusions can be drawn based on the simulation results presented; it is observed that quadratic phase-coupling *must* be present for suppression of the amplitude at the fundamental frequency of 0.17 Hz. In the case of the Rossler oscillator under periodic closed-loop control, there are many sharp frequency peaks due to the phase coherence; however, the presence of the forcing frequency maintains the conditions for forced frequency entrainment. By manually increasing the gain, k, we are in fact overcoming the self-frequency entrainment. It appears as if the QPC (Figs. 12 and 13) are being pushed to the lower frequencies and pushed to higher frequencies on the other either side of the decoupled bandwidth. Forcing the system with a constant frequency under closed-loop control, produces quadratic phase-coupling and decoupling along lines of constant frequency (related to those found in the frequency spectrum) that are perpendicular to the diagonal of the bicoherence matrix. These results show via simulation that the mechanism of synchronization consists of two sub-mechanisms, namely frequency entrainment and quadratic phase-coupling. *Both* sub-mechanisms *must* be present for synchronization to occur. Complete synchronization is indicated by a single peak in the frequency spectrum and a period-1 orbit in the phase-plane. From the closed-loop bifurcation diagram, it has been shown that by increasing the feedback gain, the system is stabilized to a limit cycle condition but the controller *does not* suppress the limit cycle; the controller cannot do so because of the *constant forcing frequency*.

6. Fixed-gain, time varying frequency control law

In this section, the results of a fixed gain-time varying frequency controller are presented. The feedback gain, k is set at 0.4. As discussed in Section 2, the forcing frequency is adjusted by a feedback loop that uses the extremum seeking control algorithm. From the frequency spectrum (Fig. 14), it can be seen that there are no distinct peaks; all the frequency peaks have been attenuated. Instead, there is frequency spreading which is centered about 0.1904 Hz (See Fig. 14). This centerline

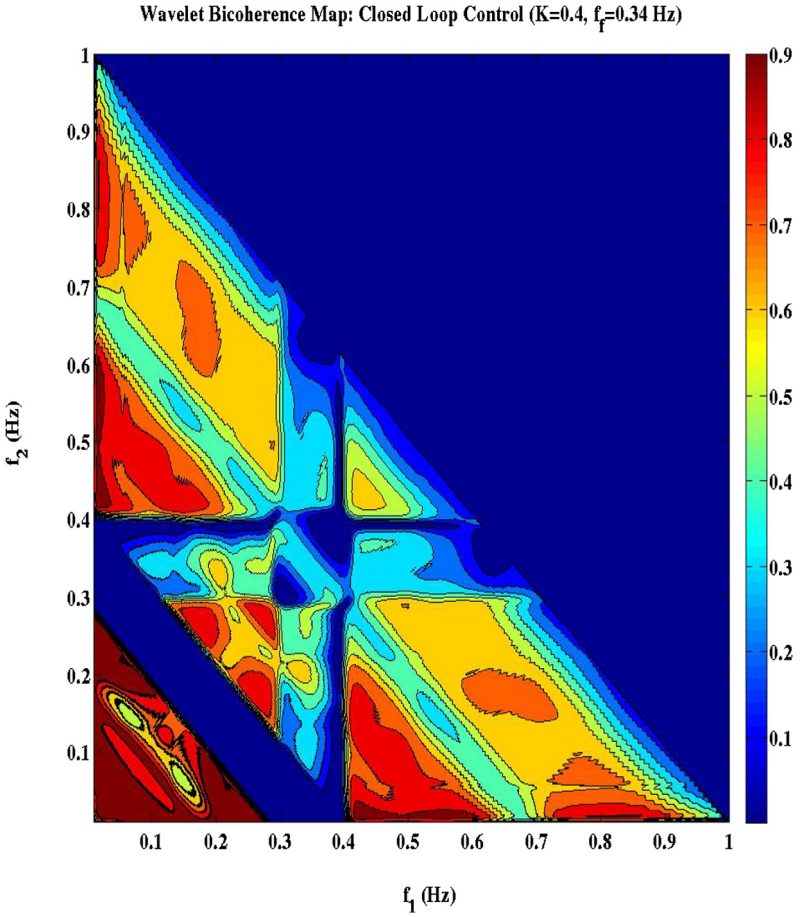

Fig. 12. Wavelet Bicoherence Map (k = 0.4 and ω_f = 0.34 Hz).

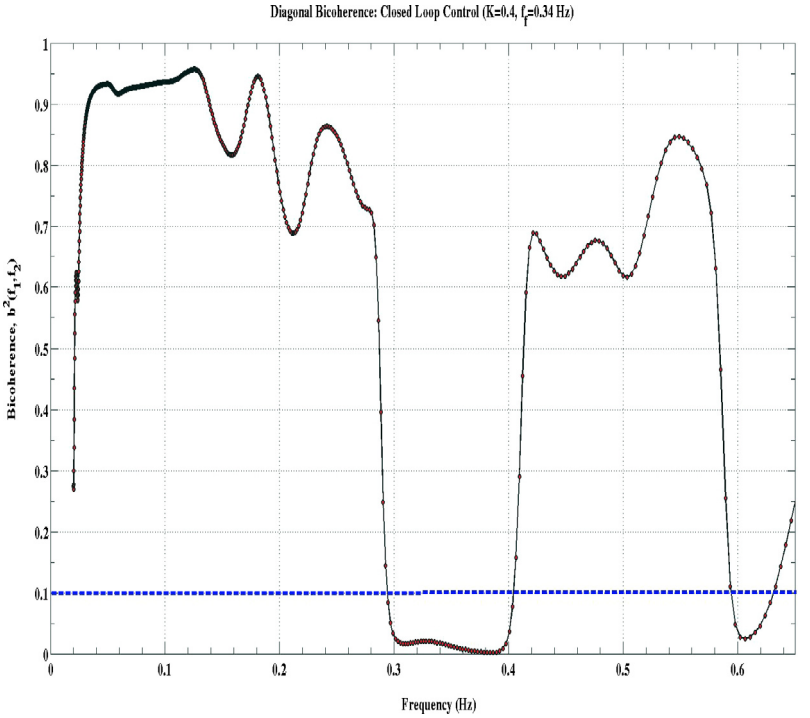

Fig. 13. Diagonal of the Bicoherence matrix ($k = 0.4$ and $\omega_f = 0.34$ Hz).

frequency is shifted by 0.02 Hz from the fundamental at 0.17 Hz. Since there are no distinct frequency peaks in the spectra, there are also no tones found in the spectrogram of the displacement in the X direction. The displacement in the X direction shows that there is intermittent periodicity (Fig. 15). The spectrogram nicely captures the spreading of frequencies (Fig. 16, bounded by the white dashed lines) seen in Fig. 16 and the intermittent periodicity seen in Fig. 15. In Fig. 15, there is a transient that last for 40 s (enclosed by the read box); the transient shows up in the spectrogram as a contraction indicated by a bright spot. A contraction in the time-frequency space is a redistribution of frequencies. Fig. 17 shows the time evolution of the forcing frequency. The white dashed line indicates the mean forcing frequency which is 0.3739 Hz. The ratio of the mean forcing frequency to 0.1904 Hz is approximately 2. The extremum seeking control loop selected a mean frequency that is slightly higher than the second harmonic. The ratio is ∼2 which suggests that the Rossler oscillator is receptive to being forced about the second harmonic; under closed-loop control it is also efficient to do so.

In Fig. 18, Lines A, B and C again represent lines of constant frequency. Line A is associated with ∼0.02 Hz. Line B is associated with ∼0.03 Hz and Line C is associated with 0.034 Hz. There is a growth in the corner due to self-coupling centered at 0.022 Hz. The magnitude of the bicoherence across these lines is shown by diagonal of the bicoherence matrix (Fig. 19). The latter shows that there are significant levels of quadratic phase-coupling at frequencies less than ∼0.06 Hz (Fig. 19, inside red box). At frequencies greater than 0.06 Hz and less than 0.2 Hz (Fig. 20), it is observed that the quadratic phase-coupling is approximately equal 0.1 indicating that there is very weak coupling. At frequencies greater than 0.2 Hz, the quadratic phase coupling is less than 0.1, indicating little to no phase coherence (as indicated by the absence of peaks in the spectra). In this case, the conditions for frequency entrainment have not been met, i.e. there are no distinct frequency peaks which means *no limit cycles*. In Fig. 14, the phase-plane demonstrates that the solution spirals *inward*. When a trajectory in a phase-plane spirals inward, it indicates that the closed-loop system is asymptotically stable. To verify this conjecture, the eigenvalues of the Jacobian matrix must be determined. The final positions of the displacements in the X and Y displacements were extracted from the data, they are (X, Y) = (0.05, 0.0145). The Jacobian matrix is linearized about this point and the eigenvalues calculated. The eigenvalues that correspond to the X and Y displacements are $-0.1109 \pm 1.1506i$. The real part of the eigenvalue is negative; this tells us that point (X, Y) = (0.05, 0.0145) is a stable attractor in the Lyapunov sense. Therefore, the closed-loop system is indeed asymptotically stable. Note that *only* linear systems can exhibit spiral trajectories.

The following observations are made based on the results presented in this section:

- The controller provides broadband attenuation due to the time varying forcing frequency and results in the suppression of the phase coherence typically found in the Rossler oscillator. Fig. 21 is a comparison between the controlled and uncontrolled phase spaces. It shows that the phase coherence preserves the eyelet feature, but by removing the conditions needed for frequency entrainment, i.e. no strong peak, the control action is able to 'collapse' the eyelet.
- The conditions for frequency entrainment are not present, and as such there can be *no* formation of a limit cycle.

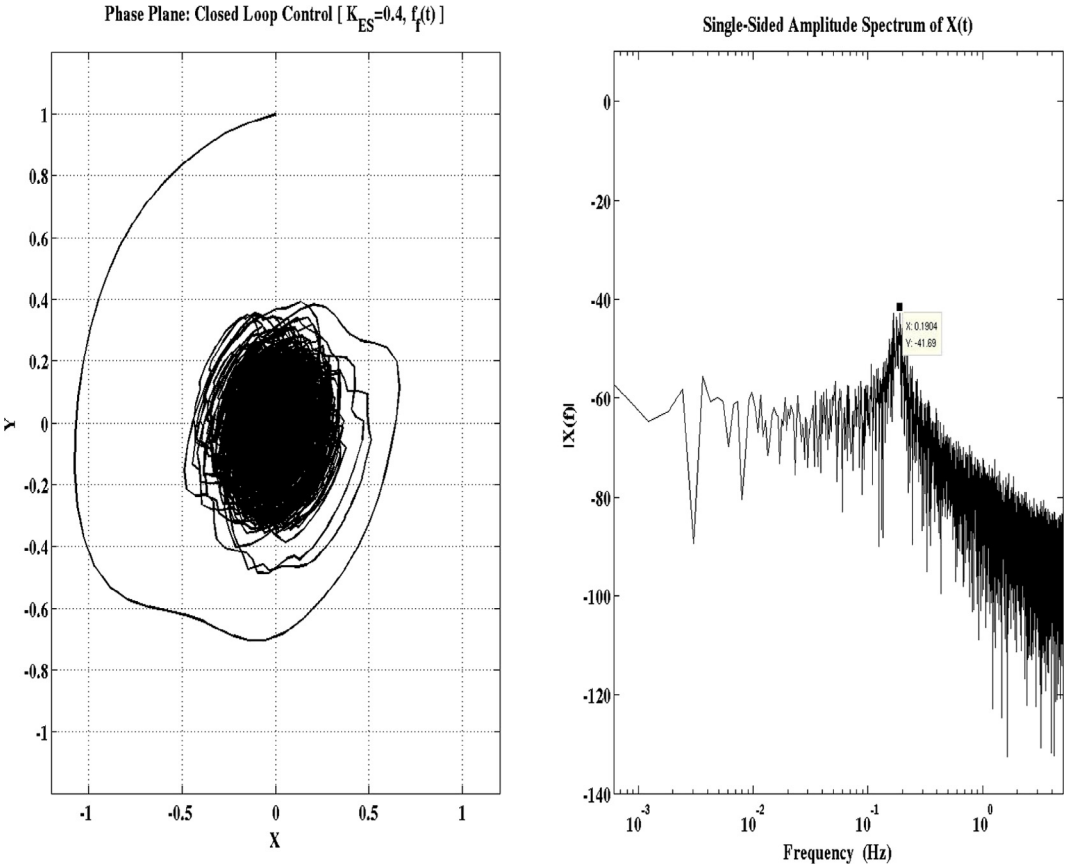

Fig. 14. Closed loop natural frequency, 0.1904 Hz (Extremum Seeking).

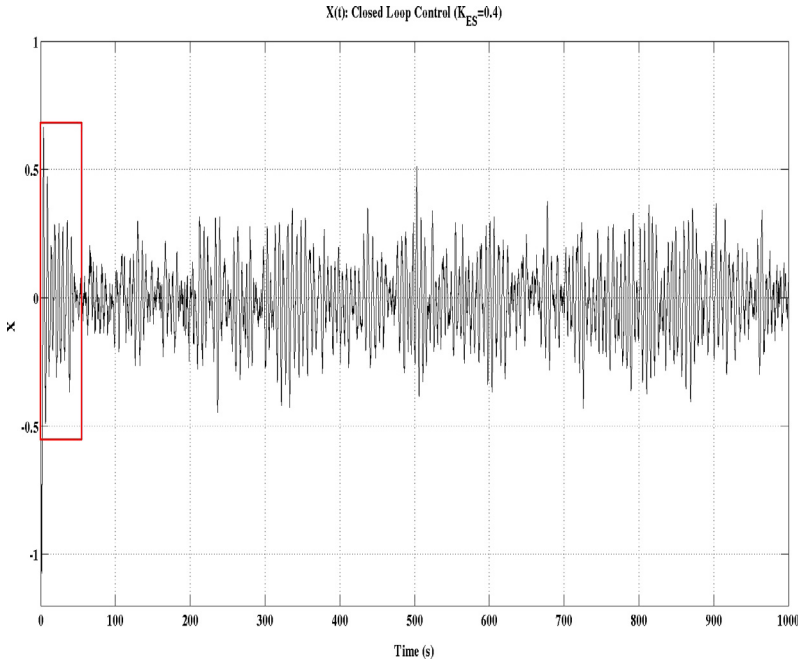

Fig. 15. Time history, X-displacement.

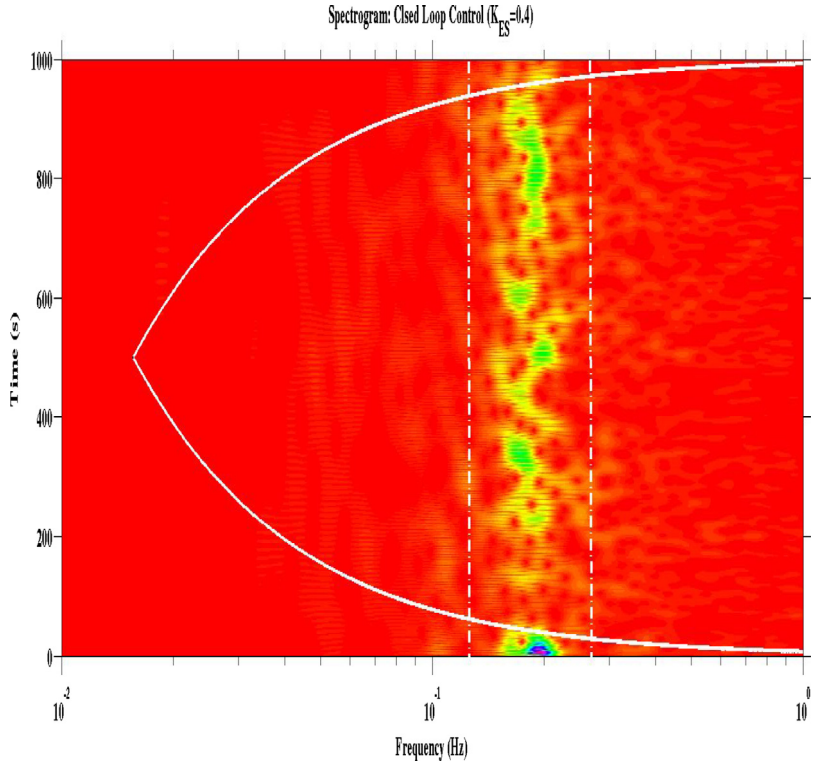

Fig. 16. Spectrogram, X-displacement (Extremum Seeking).

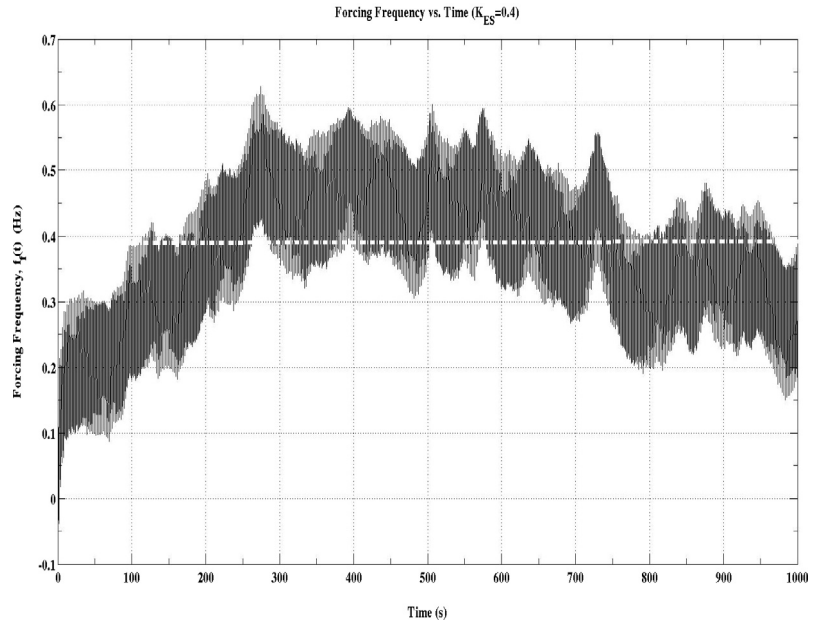

Fig. 17. Time History, Forcing Frequency.

- Quadratic phase-coupling is strongly induced by the control action and only present at frequencies less than 0.2 Hz in the system as evidenced by the attenuation of the system frequencies.
- Varying the forcing frequency with time has the effect of 'linearizing' the Rossler oscillator as evidenced by the phase-plane trajectory converging to a point and the significant reduction in quadratic phase-coupling at frequencies greater than 0.2 Hz (Fig. 19). The system is said to be asymptotically stable.

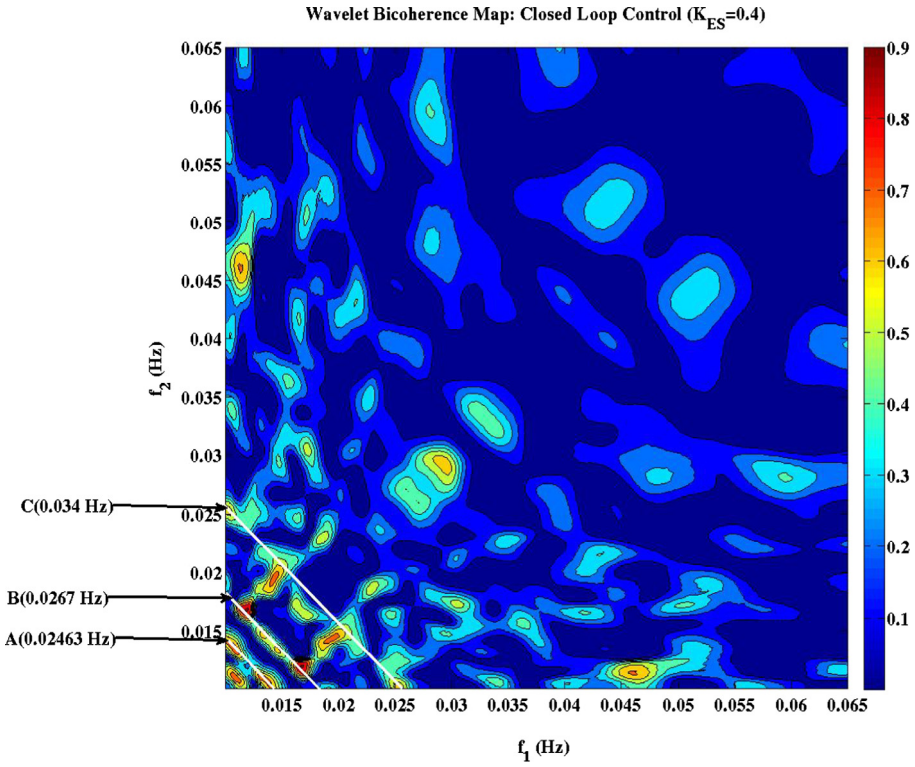

Fig. 18. Wavelet Bicoherence Map (Extremum Seeking).

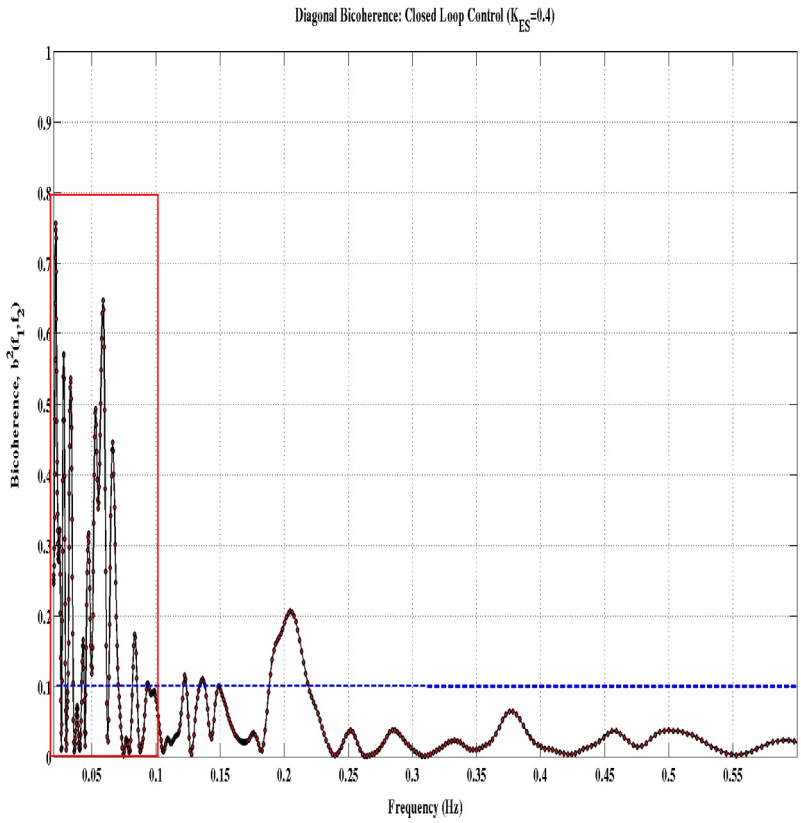

Fig. 19. Diagonal of the Bicoherence matrix (Extremum Seeking).

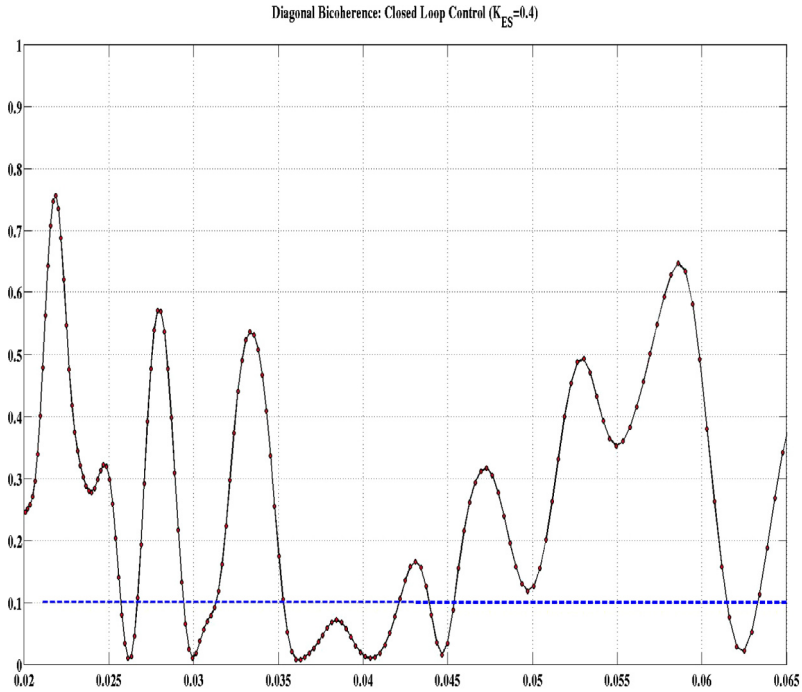

Fig. 20. Region enclosed by the red box in Fig. 19, Note the high b^2 at $f < 0.06$ Hz.

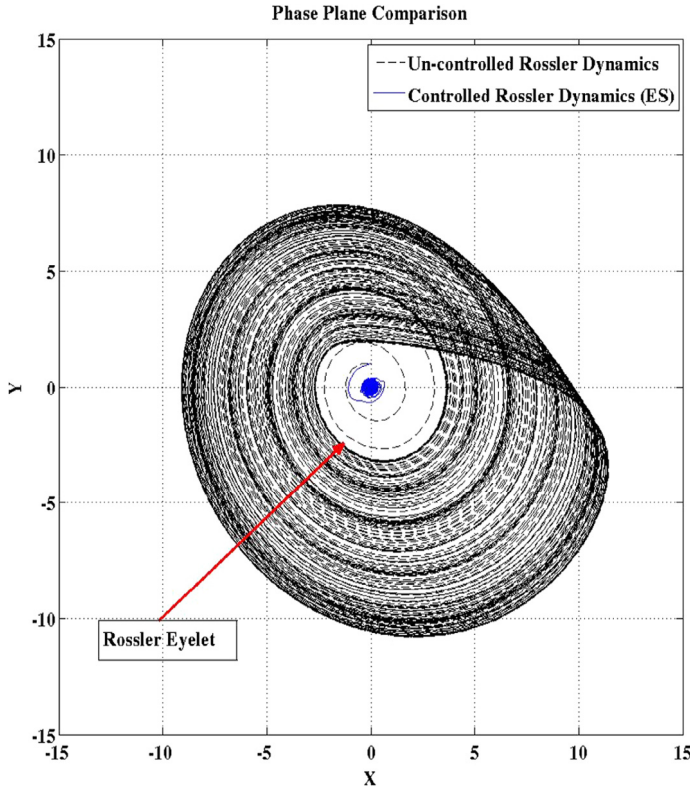

Fig. 21. Phase-plane comparison.

Lastly, quadratic phase-coupling is still present, but there is no frequency entrainment and hence no limit cycle as stated above; this means that effectively, there is no synchronization present in the closed-loop system. However, the controller has successfully suppressed the chaotic response without synchronization.

7. Conclusion and future research

It has been shown via simulation that the mechanism of synchronization consists of two sub mechanisms, namely frequency entrainment and quadratic phasecoupling. Both sub-mechanisms must be present in order for there to be synchronization. For the fixed-gain, fixed-frequency controller, frequency entrainment with quadratic phase-coupling stabilizes the Rossler system to a limit cycle; the conditions for frequency entrainment must be met in order to have synchronization. The fixed gain-fixed frequency controller *cannot* suppress a limit cycle with a constant forcing frequency. The auto-bispectral analysis has shown that the fixed-gain, fixed-frequency controller generates decoupling bandwidths and bandwidths of high quadratic phasecoupling to suppress the chaotic response but enable the formation of a limit cycle.

For the fixed-gain, time-varying frequency controller (with extremum seeking), it has been shown that the time-varying forcing frequency 'linearizes' the system. The controller attenuates all frequencies, thereby removing the strong frequency peak needed for frequency entrainment. Since there is no frequency entrainment, there can be no limit cycle. As such, only the sub-mechanism of quadratic phase-coupling remains. The controller achieves suppression without synchronization as evidenced by the collapse of the Rossler eyelet. These results show in a simple manner the potential for further application of bispectral analysis as a diagnostic tool for controlled mechanical and aeromechanical systems. For instance, it would be interesting to examine practical nonlinear systems under open and closed-loop control such as lifting surface aerodynamic flows (active flow control), aeroservoelastic systems (as mentioned earlier), vibration suppression control laws and algorithms for the suppression of pilot induced oscillations (PIOs). Lastly, it should be noted that wavelet based bispectral analysis in its mathematical current form cannot detect linear couplings in a single measurement; bispectral analysis implicitly detects the presence of linear couplings when the magnitude of the bicoherence is significantly below $\sim$0.1.

Acknowledgements

This work was originally supported by the U.S. Airforce Office of Scientific Research (AFOSR) and Clarkson University and currently a MITACS Accelerate Post-Doctoral Fellowship at the University of Sherbrooke. The authors would like to thank the AFOSR and greatly appreciate the support from Dr. Stephane Moreau and the University of Sherbrooke Aeroacoustics Group.

Appendix A. Schematic of extremum seeking controller

See Fig. A1.

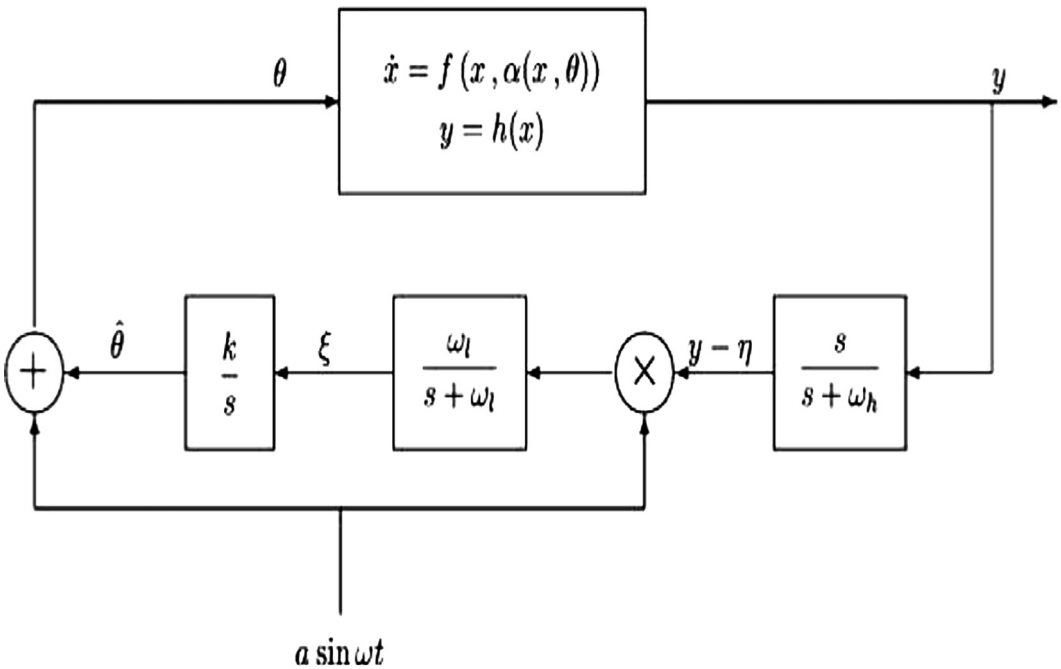

Fig. A1. General block diagram for extremum seeking controller [7].

References

[1] C. Pezeshki, S. Elgar, R.C. Krishna, Bispectral analysis of possessing chaotic chaotic motion, J. Sound Vib. 137 (3) (1990) 357–368.
[2] C. Pezeshki, S. Elgar, R.C. Krishna, T.D. Burton, Auto and cross-bispectral analysis of a system of two coupled oscillators with quadratic nonlinearities possessing chaotic motion, ASME J. Appl. Mech. 59 (1992).
[3] K.A. Khan, B. Balachandran, Bispectral analysis of interaction in quadratically and cubically coupled oscillators, Mech. Res. Commun. 24 (5) (1997) 545–550.
[4] M. Pasquali, W. Lacarbonara, P. Marzocca, Detection of nonlinearities in plates via higher-order-spectra: numerical and experimental studies, J. Sound Vibrations 136 (2014) 041015.
[5] Muhammad R. Hajji, Walter A. Silva, Nonlinear flutter aspects of the flexible HSCT semispan model, in: AIAA-2003-1515, 44thAIAA/ASME/ASCE/AHS/ASC Structures, Structural Dynamics and Materials Conference, April 7-10, Norfolk, VA, 2003.
[6] Christopher C. Chabalko, Identification of Transient Nonlinear Aeroelastic Phenomena Doctoral Dissertation, Virginia Polytechnic Institute and State University, 2007.
[7] Kartik B. Ariyur, Miroslav Krstic, Real-Time Optimization by Extremum-Seeking Control, Wiley Interscience, 2003.
[8] Farmer, Doyne, Crutchfield, James, Froehling, Harold, Packard, Norman and Shaw, Robert, Power spectra and mixing properties of strange attractors, Annals of the New York Academy of Sciences, Nonlinear Dynamics, vol. 357, 1980, pp. 453–471.
[9] Emily F. Stone, Frequency Entrainment of a phase coherent attractor, Phys. Lett. A 163 (1992) 367–374.
[10] H.C. Gilliatt, T.W. Strganac, A.J. Kurdilla, An Investigation of Internal Resonance in Aeroelastic Systems, Springer Nonlinear Dynamics No. 31, 2003, pp. 1–22.
[11] D. Iatsenko, P.V.E. McClintock, A. Stefanovska, Linear and synchrosqueezed time-frequency representations revisited. Part I: Overview, standards of use, related issues and algorithms, submitted to Dig. Signal Proc., Pre-print [arXiv: 1310.7215], Oct. 2013.
[12] Robert Bruce Alstrom, Aerodynamic Flow Control of a High Lift System with Dual Synthetic Jet Arrays Doctoral Dissertation, Clarkson University, 2013.
[13] Janez Jamsek, Stefanovoska, P.E.V. McClintock, Khovanov, A. Igor, Time-phase bispectral analysis, Phys. Rev. E 68 (2003) 016201.
[14] Janez Jamsek, Stefanovoska, P.E.V. McClintock, Nonlinear cardio-respiratory interactions by time-phase bispectral analysis, Phys. Med. Biol. 49 (2004) 4407–4425.